

Frequency Reconfigurable Multiband Antenna for IoT Applications in WLAN, Wi-Max, and C-Band

Prem P. Singh¹, Pankaj K. Goswami^{2,*}, Sudhir K. Sharma¹, and Garima Goswami³

Abstract—Due to the upsurge in internet connected devices in everyday life, a compact embedded wireless device becomes essential to cater multiple frequency-based applications at common platform. Reconfigurability is the best solution to enhance the device utility at many technical interfaces. Wireless compatibility among different devices via internet elicits the importance of antenna unit. In this paper, a compact size $25 \times 25 \text{ mm}^2$ ($L_{Sub} \times W_{Sub}$), five-band frequency reconfigurable antenna is presented. The antenna exhibits the choice-based optimized frequency responses of slot structures, corner truncation, and parasitic loading. These individual responses comprise the high frequency switching characteristics in synchronized module of three PIN diodes. The antenna is designed to operate among five different frequencies, i.e., 3.85 GHz, 4.14 GHz, 4.43 GHz, 4.91 GHz, and 6.01 GHz. The work emphasizes the compact design and wide switching ability of the antenna, which validates its unique feasibility for high speed multiple applications of Internet of Things (IoT) through a common embedded platform under WLAN, Wi-Max, and C-band applications as per the FCC standards.

1. INTRODUCTION

Compact size antennas have attracted researchers for extended applications due to small size, light weight, and ease of fabrication. Patch antenna can be used in remote accessing of radar, missiles, and aircraft applications with high fidelity and compact structure [1]. The tremendous changes in the area of communication have increased the need of multipurpose and multi-application devices [2]. As the electromagnetic spectrum is a limited resource, the antenna must be flexible as well as easily adaptable to different practical situations. Thus, reconfigurable antennas are highly suitable for advancing e-utility applications. The internet of things (IoT) and Industrial Internet of Things (IIoT) are on top priorities for next stage modification and implementations. This develops the need of a wireless system, which can provide a common functional platform for multiple applications. An embedded system with frequency reconfiguration properties may lead to design analyst to a step ahead in utility enhancement. A compact size antenna, with frequency-reconfigurable property and circular polarization, deserves as an adequate system essential. Reconfiguration may be achieved in any property such as frequency, polarization, and radiation pattern. Frequency reconfigurable antennas can reduce the requirement of large bandwidth and vast frequency spectrum allotment. Frequency reconfigurability can be obtained by varying the distribution of surface current of the radiating structure [3]. The antenna can be reconfigured in frequency by using PIN diodes, RF-MEMS switches, and varactors. In [4], a frequency reconfigurable antenna is proposed for LTE applications operating from frequency of 0.9 GHz to 3.5 GHz. PIN diodes are used for reconfiguration purpose with area of $50 \text{ mm} \times 60 \text{ mm}$. A hex band frequency PIN diode switching based reconfigurable antenna for wireless communication operates in 2.18 GHz to 5.2 GHz with

Received 25 February 2020, Accepted 6 May 2020, Scheduled 26 May 2020

* Corresponding author: Pankaj Kumar Goswami (g.pankaj1@gmail.com).

¹ Department of Electronics and Communication Engineering, Jaipur National University, Jaipur 302017, India. ² Department of Electronics & Communication Engineering, Teerthanker Mahaveer University, Moradabad 244001, India. ³ Department of Electrical Engineering, Teerthanker Mahaveer University, Moradabad 244001, India.

three PIN diodes [6]. A fractal shaped antenna is reconfigurable with multiband characteristics and uses a number of PIN diodes [7]. Therefore, many techniques are available to achieve the reconfigurability of an antenna, but at the same time the compactness of the antenna is equally essential. Meanwhile, an antenna for IoT and IIOT systems must follow data transfer rate protocols and should have orientation free surfaces. Those complexities develop the scope of improvement and design analysis. The design analysis concludes the design attributes as compact size, adequate frequency bands for maximum utility such as Wi-Fi, Wi-Max, frequency reconfiguration, circular polarization, efficiency, and gain of the antenna. Among all the essential attributes, frequency reconfiguration and circular polarization are chosen as core independent essentials, and the rest are adjusted as optimum offsets [8–11]. The research reported the use of high-speed switching devices to make structure reconfigurable, but at the same time the system ambiguities also increases. This contains a deep empirical review of previous work to elicit the attributes of an antenna for IoT systems. In [12], a reconfigurable antenna with frequency reconfiguration is proposed with loading of 6 PIN diodes with large area of $40\text{ mm} \times 40\text{ mm}$ and frequency range from 2.35 to 3.46 GHz. The key challenge of designing frequency reconfigurable patch antennas is to realize compact structures while maintaining similar radiation patterns at all the operating frequencies with satisfactory performance. In [13], a patch antenna is reported for wireless LAN applications with two PIN diodes as a switching device in the structure, and the antenna is tuned for 2.4 to 5.2 GHz. A quad-band monopole patch antenna is designed with the use of two PIN diodes and folded strip lines with DGS structure. This explores the opportunity of symmetrical multi-fold strip lines for obtaining the distinguish bands [14, 15]. Also, in [16] a tunable antenna for cognitive radio is presented using a varactor diode with a slotted grid and elicits the technical utility of the varactor diode for frequency tuning in range 2.45–3.55 GHz. Three and four PIN diode configurations are widely used for obtaining reconfiguration properties with sustainable radiating characteristics in Wi-Max, WLAN, and GPS systems. An antenna size ($60 \times 65\text{ mm}^2$) is a great constraint in many available smart applications over the discussed range of operating frequency [17, 18]. A compact size antenna with minimum need of surface mounts devices SMD to achieve reconfigurability. Additionally, in IoT applications more emphasis is required to improve signal quality, bandwidth, efficiency, device compatibility, and interfacing. A high-fidelity antenna system for ultra large band application is suggested for smart wireless IOT sensors [19]. In this paper, a compact frequency reconfigurable patch antenna operating on five different frequencies is presented for smart internet of things applications-based devices. The main contributions comprise the compactness of the structure along with faster switching between the two transition bands. The antenna satisfies the multiple frequency-based applications from a common embedded system to explore new opportunities and extensions in IoT systems.

2. ANTENNA DESIGN

2.1. Antenna Systems for IoT Modules

Patch antennas are generally used in IoT devices and have GPS capabilities as signals transmitted from the satellite are often either right-handed circular polarization (RHCP) or left-handed circular polarization (LHCP). Patch antennas have the capability of dual polarizations which can be reconfigured by switching a perturbation element using PIN diode, varactor diode, or RF-MEMS switches, but there are still many patch antennas that operate only for one type of polarization between linear, LHCP, or RHCP. Many times, it is difficult to choose the perfect type of polarization matching the transmission. IoT devices in which antennas like chip and PCB have been embedded have benefit that they can be fit in a small area, shrinking a sensor node's dimensions. PCB antennas composed of conductive traces exhibit higher gains than their chip-based counterparts. Figure 1 shows a basic three-layer IoT design architecture, which has a basic three-layer design module consisting of user defined applications, network protocols & securities, and perception & control layers. The perception layer facilitates accessing and recording of all the data availability of the system; therefore, an efficient system is essentially required to perceive signal data with efficient data rate control.

There are many antenna topologies available for PCB antenna such as inverted-F, L, and folded monopole [19]. Ground plane also has importance in the development of chip antennas. A smaller ground plane can limit the design significantly having a narrower bandwidth and improved radiation pattern. As for any antenna the radiator's volume is directly proportional to its gain, and embedded

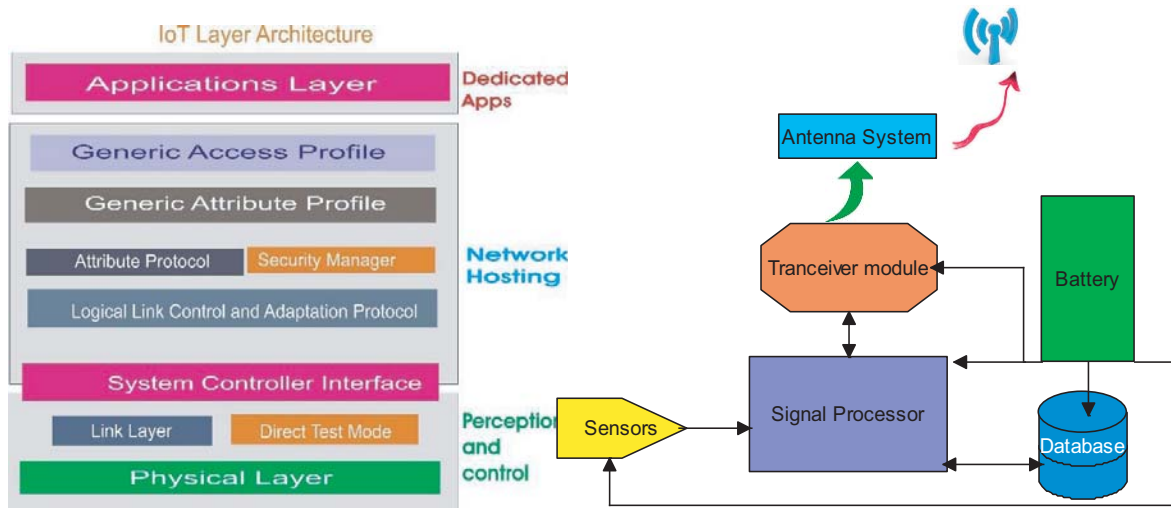


Figure 1. IoT system architecture and signal perception.

chip antennas occupy lots of space on the board. However, sensor nodes having a PCB antenna have the characteristic of keeping a regular shape that could allow easier enclosing and mounting in any environment. Table 1 shows various frequency applications of IoT devices and antenna feasibility to facilitate such wireless communication [20]. Directional antennas such as Yagi and sectorial antennas can be used either to extend a radiation range or for IoT base stations. The mechanical fluctuation of high-gain directional antennas provides a larger communication distance than omnidirectional antennas. Yagi antennas are generally used in Supervisory Control and Data Acquisition (SCADA) system for IoT that allow increased data rate and also reliability. Sector antennas usually exhibit a wider beamwidth than Yagi antennas.

Table 1. Frequency spectrum of IoT applications.

Technology	Frequency	IoT Applications
Zigbee	915 MHz, 2.4 GHz	General (Smart Home/Commercial buildings)
Z-Wave	2.4 GHz	
Bluetooth	2.4 GHz	
Wifi	2.4 GHz, 3.6 GHz, 4.9 GHz, 5 GHz and 5.9 GHz	
Wireless HART	2.4 GHz	IIoT
ISA 100.11a	2.4 GHz	
MBAN	2360–2400 MHz	Medical
WBAN	2.4 GHz	
WAIC	4200–4400 MHz	Avionics

Table 2 shows the basic attributes and risk analysis of IOT systems, which indicates the precise data rate and system adherence as a key aspect of the design analysis. This elaborates the need of fast switching devices to function among the sequenced IOT primitives. Moreover, effective transmission and control require the risk analysis in IoT system on the basis of design primitives. Sequentially, perception layer elicits physical layer sensor attributes with high probability of false

Table 2. Attributes in IoT systems.

IoT primitives	Aspect	Aristocratic Risk?	Reliability Risk?	Security Risk?
Sensor	Physical	Y	Y	Y
Aggregator	Virtual	Y	Y	Y
Communication channel	Virtual and/or Physical	Y	Y	Y
e-Utility	Virtual or Physical	Y	Y	Y
Decision trigger	Virtual	Y	Y	Y

triggering risk in all three (aristocratic, reliability and security) categories. On virtual or physical integrated development environment (IDE), communication channels and remote accessing experience high threat equally. The decision trigger is end user interface (EUI), which leads all the RF stimuli and elicits challenging attributes to deal RF access risk attributes. This develops the eventual need of effective RF perception and secure sensor attributes in IoT systems in both physical & virtual layers. The adequate reconfigurability of an RF perception device (antenna) can reduce the threat of unwanted interference and enhance the system reliability in IoT devices. This paper contributes towards the elementary frequency reconfiguration of antenna with adequate competence of sensors aggregators and communication channels to enhance the e-utility.

2.2. Proposed Design Strategy

The modified reconfigurable antenna module is shown in Figure 2. The antenna has the effect of fractal stripping and rectangular slotted geometry. The ground plane is also defected with an Inverted-U slot of length (S) and two ring slots. Frequency reconfiguration is proposed through simultaneous switching of three PIN diodes among surrounded parasitic structures and radiating patch. One PIN diode is used in the U slot in ground to vary equivalent inductance and capacitance. The other two PIN diodes are connected between center radiating patch and the parasitic strip of length P_1 . Additionally, the ground plane is loaded with two parallel closed rectangular slot structures, eventually two parallel rectangular parasitic strips. This variation leads to tuning of impedance matching and optimizing the equivalent

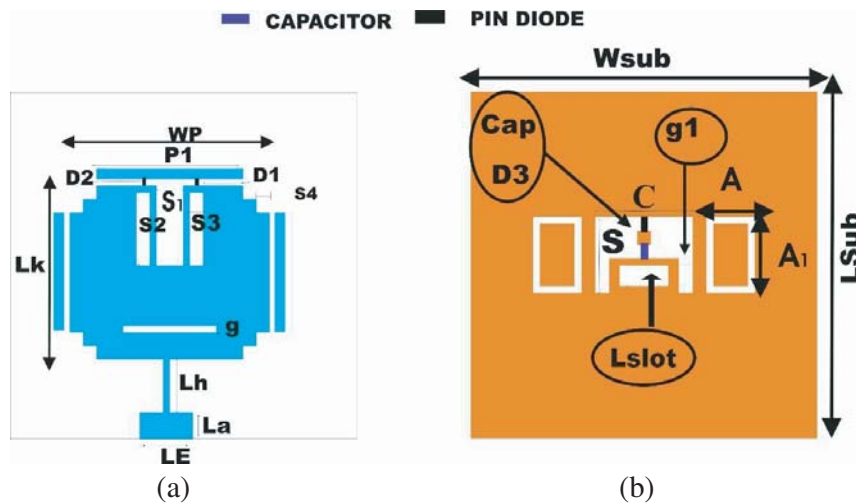


Figure 2. Geometry of proposed antenna. (a) Top view. (b) Bottom view.

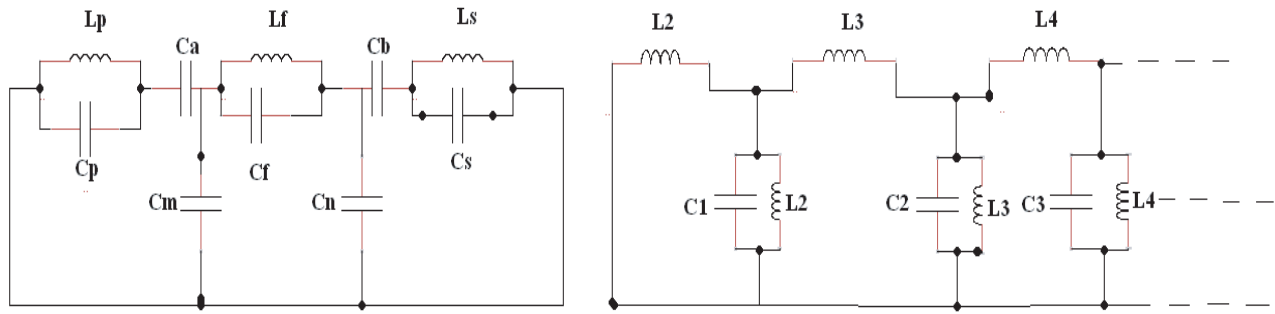


Figure 3. Equivalent diagram under on/off condition.

resonant circuitry in desired operating area. The antenna prototype is fabricated on a $25 \times 25 \text{ mm}^2$ FR-4 substrate with dielectric constant $\epsilon_r = 4.4$ and thickness 1.6 mm. This is possible using electronic or mechanical switches such as PIN diodes, varactor diode, and RF-MEMS switches. Here, PIN diodes are used as a prime switching device, and the combination of state of PIN diodes makes the structure reconfigurable. BAR50-02V PIN diodes from Infineon technologies are preferred for stable switching and necessary transient response. A capacitor is used in the ground to avoid the problem of shorting of DC supply. Conceptually, varying current distribution causes the variation in radiating area and hence, radiating frequency. Also, the immediate switching significantly varies the net impedance of the structure. Figure 3 shows the two states of the structure equivalence under ON and OFF conditions. Under ON switching the respective circuit indicates that shunt connections of inductive and capacitive loading are indicated by L_p, L_f, L_s and C_p, C_s, C_f , while coupling capacitance is connected in series and shunt connections as C_a, C_b and C_m, C_n consecutively. The impedance orientation reverts during OFF state of PIN diode, which results in parallel tank circuits $(C_1, L_2), (C_2, L_3)$, and so on with coupling inductances to vary over all impedance of the patch surface. The conditional antenna equivalence develops varying impedance bandwidth and impedance matching shifts. Respective frequency shifts are elicited through parallel and series combinations of patch reactance by current path orientation via PIN switching transitions. This variation leads to the main scheme of obtaining reconfiguration through multimode impedance matching. The reconfiguration mechanism depends upon the diode switching as in ON state PIN diode acts as series combination of resistance $R_s = 3 \Omega$ & inductance $L = 0.6 \text{ nH}$, and in OFF state it acts as parallel combination of capacitance $C_p = 0.15 \text{ pF}$ & resistance $R_p = 5 \text{ k}\Omega$ with series inductance of 0.6 nH .

The equivalent circuit of PIN diode is shown in Figure 4. Different parameters of antenna geometry and dimensions are given in Table 3. For the given PIN diode, the values of resistance, capacitance, and inductor for ON and OFF state are given in Table 4. In OFF state, the capacitor blocks the current, and there is no current flow in this case, thus it works as an open circuit.

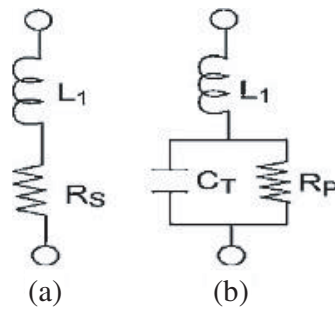


Figure 4. PIN diode equivalent diagrams. (a) ON state. (b) OFF state.

Table 3. Dimensions of antenna.

Parameter	Dimension (mm)	Parameter	Dimension (mm)
W_{Sub}	25	P_1	11
L_{Sub}	25	g	0.5
W_p	15	S_4	1
L_k	13	A	3.5
L_h	4	L_{Slot}	1.5
L_a	2	$S = S_2$	5.5
L_E	4	$g_1 = S_1$	1
C	7	A_1	5.5

Table 4. PIN diode BAR50-02V.

PIN Diode Model	State	L	C_T	R_P	R_S
BAR50-02V	OFF		0.15 pF	3 k Ω	
	ON	0.6 nH			3 Ω

3. RESULTS AND DISCUSSION

The design antenna undergoes several iterations based on return loss characteristics and other crucial parameters. The initial structure is evolved from a $15 \times 13 \text{ mm}^2$ rectangular patch followed by the design rule of antenna modelling. Later, structured slot analysis and advanced iterative modelling help to obtain the proposed shape of the antenna. Figure 5 shows the effect of consecutive modifications and slotted structures as return loss characteristics. Results in this section elicit the effectiveness of parallel slots and parasitic strips without high frequency switching. Approximately, 900 MB impedance bandwidth is achievable through the entire process of slot insertion at appropriate location and parasitic loading. The antenna is highly feasible for operating frequencies 3.85 GHz, 4.14 GHz, 4.43 GHz, 4.91 GHz, and 6.01 GHz in the domain of multifold categories of IoT based application. The utility of the antenna becomes novel with reusable frequency applications and offers more application by a single unit of antenna. Among various available resources, PIN diode switching exhibits more stable response and better transient frequency shift. Technically, PIN diode is compatible for large range of microwave frequency and satisfies the radiating possibilities of the structure. The novelty of this work is in the positioning and concurrent switching of three switching diodes to force antenna to operate in desired frequency band. Based on the combinational switching sequence of diodes, antenna exhibits

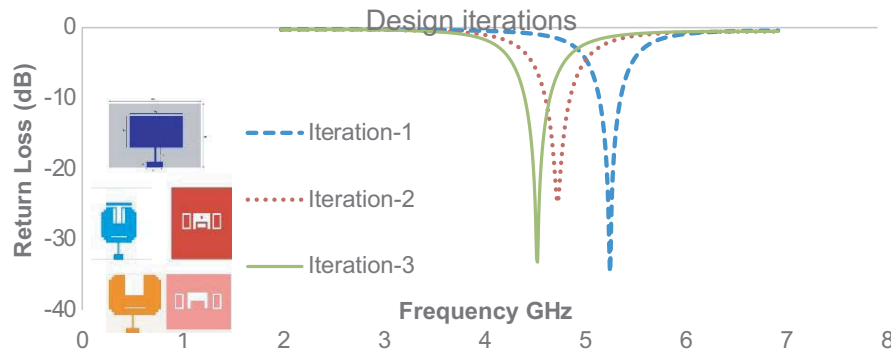
**Figure 5.** Design iterations and respective return losses.

Table 5. Configurations of diodes.

D ₁	D ₂	D ₃	State
OFF	OFF	OFF	000
OFF	ON	ON	001
ON	OFF	OFF	110
ON	ON	ON	111

frequency reconfiguration. The four best possible combinations of three PIN diodes are as given in Table 5.

Here ‘0’ indicates diode in OFF state, and ‘1’ indicates ON state. To operate the antenna for different frequencies and bands, the electrical lengths and current densities need to be varied. An additional strip of 10 mm is used which acts as a parasitic element in the absence of PIN diode. It is found that the parasitic element can increase the antenna bandwidth and change the radiation resistance. To understand the operating principle of antenna, it would be helpful to analyze the current distribution according to the switching states of PIN diodes. The return loss for different combinations of PIN diodes is plotted in Figure 6. In the first case, when all the diodes are in OFF state, the antenna acts as dual bands and radiates on two frequencies of 4.14 GHz and 6.01 GHz. In this combination, all the diodes are OFF; therefore, only the central patch radiates, and rest of the side strips exhibit the mutual coupling with active radiator. Similarly, various ON-OFF combinations of D1, D2, & D3 diodes alter the effective electrical length of the patch and current distribution in radiating surface. At lower frequency, the current distribution covers larger area of patch so that the electrical length is equal to $\lambda/4$. This elaborates that the resonant frequency shift towards higher side increases when the radiating part decreases.

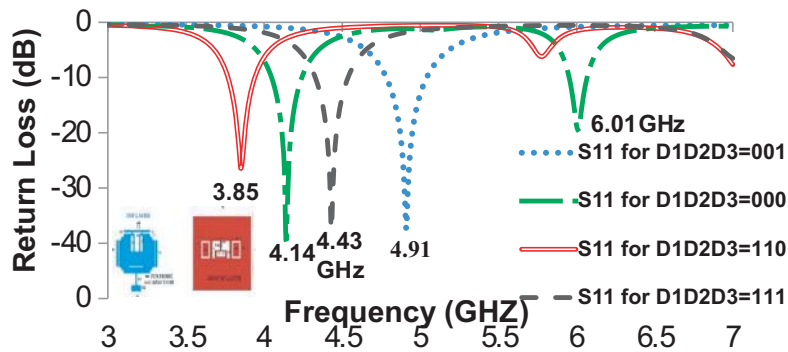


Figure 6. Frequency reconfiguration in (dB).

Figure 7 shows the effective current distribution during all possible modes of switching operations. This specifies the radiating strength of the various associated antenna strips and created slots. The PIN diode offers transition from high impedance state to low impedance state in a certain part of current carrying surface. The passive lumped L-C network varies through altered series & parallel combinations via various pin diode switchings. In the second case, diode D1 and D2 are OFF, and D3 is ON, i.e., 001 state. In this case, the effective area of the ground is changed and thus the operating frequency of the complete structure also varied. The operating frequency in this case is 4.91 GHz with S_{11} of 37.5 dB. It can be observed that the resonant frequency decreases as the radiating part increases or vice-versa.

In the third case when diode D1 and D2 are ON, and D3 is OFF, the antenna operates on 3.85 GHz with return loss of 26.85 dB and VSWR of 1.14. In this combination, the parasitic strip above the patch is directly connected to the patch, and thus the effective radiating area is increased. Due to this the operating frequency shifts to lower edge of frequency.

When all three diodes are in ON condition, the antenna radiates on 4.43 GHz with return loss

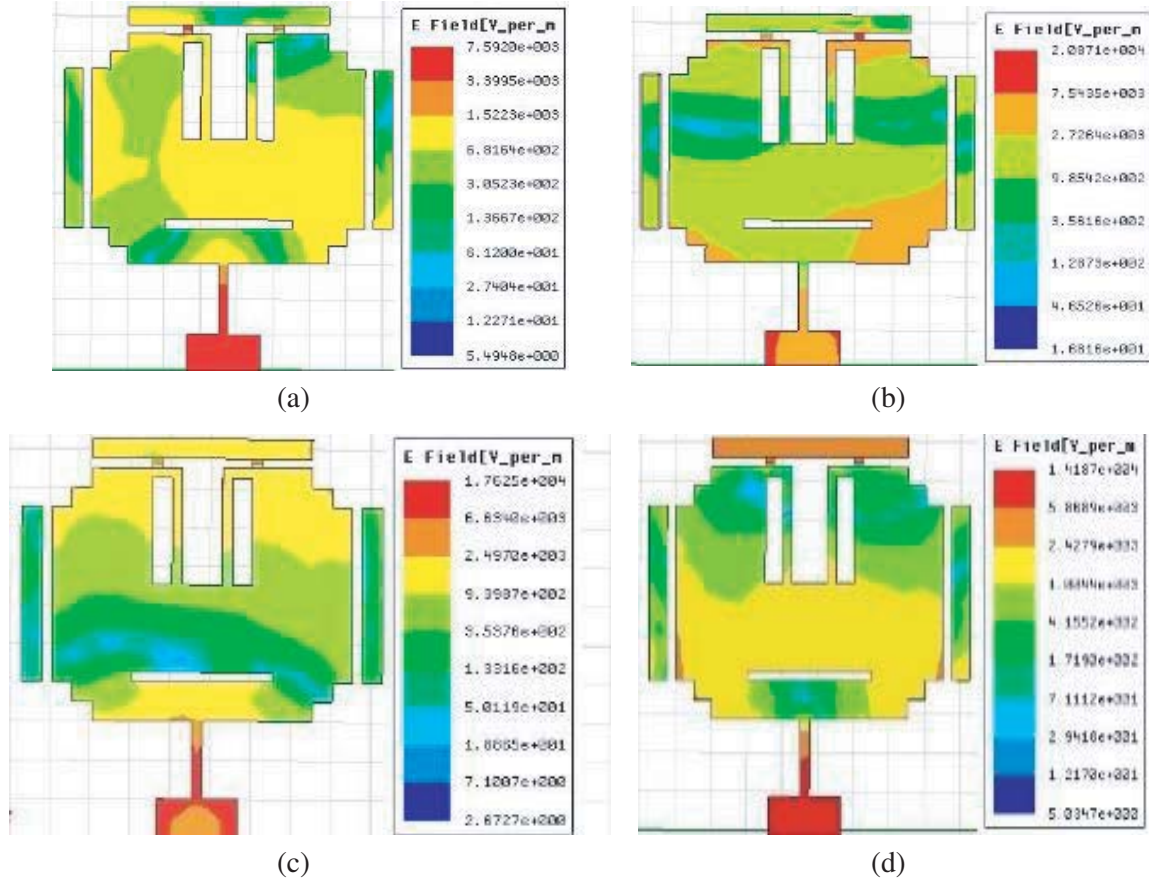


Figure 7. Electric field current distribution. (a) 4.14 GHz ($D_1D_2D_3 = 000$). (b) 4.91 GHz ($D_1D_2D_3 = 001$). (c) 3.85 GHz ($D_1D_2D_3 = 110$). (d) 4.43 GHz ($D_1D_2D_3 = 111$).

value of -37.54 dB, and VSWR is 1.06 at resonant frequency. By switching the diodes ON in ground frequency gets shifted to 4.43 from 4.14 GHz. In the third case, the antenna operates on 4.14 GHz, and in the fourth case, the diode D_3 is also turned ON from OFF so that frequency shifts to 4.43 GHz. The values of S_{11} parameters for 4.14 GHz and 6.01 GHz are -39.43 dB and -19.48 GHz, respectively, and efficiencies are 54% and 63% for 6.01 GHz and 4.14 GHz, respectively. The return loss parameters for all diodes D_1 , D_2 , and D_3 in OFF state are shown in Figure 8. The antenna prototype is fabricated using commercially available FR4 material with dielectric constant 4.4 and thickness 1.6 mm. The PIN diodes are biased with an external dc biased circuit with on/off switching. The measured and simulated results offer a good compromise to validate the structure for real time application. The realized gain of the antenna over the frequency range appears stable and lies with an average value of 2.1 dBi for the entire range. Figure 9 shows the experimental setup of measurement of return loss characteristics of the proposed antenna under different switching conditions.

The use of DC supply for the biasing of PIN diodes affects the RF current and provides an alternative track to flow the RF current [21]. So to remove the problem, i.e., to stop the flow of RF current through the DC lines, the RF choke inductors are necessary to be inserted between the diode and DC supply. The well-known feature of an inductor is to stop AC current from flowing and pass the DC current. The value of the inductor used in a DC biasing circuit can be calculated at the minimum operating frequency, i.e., 3.85 GHz. The impedance X_L must be high to block the flow of AC current, i.e., greater than 1 k. The value of inductor impedance used here is 2.5 k Ω .

$$X_L \geq 1 \text{ k} \quad (1)$$

$$X_L = 2\pi fL \quad (2)$$

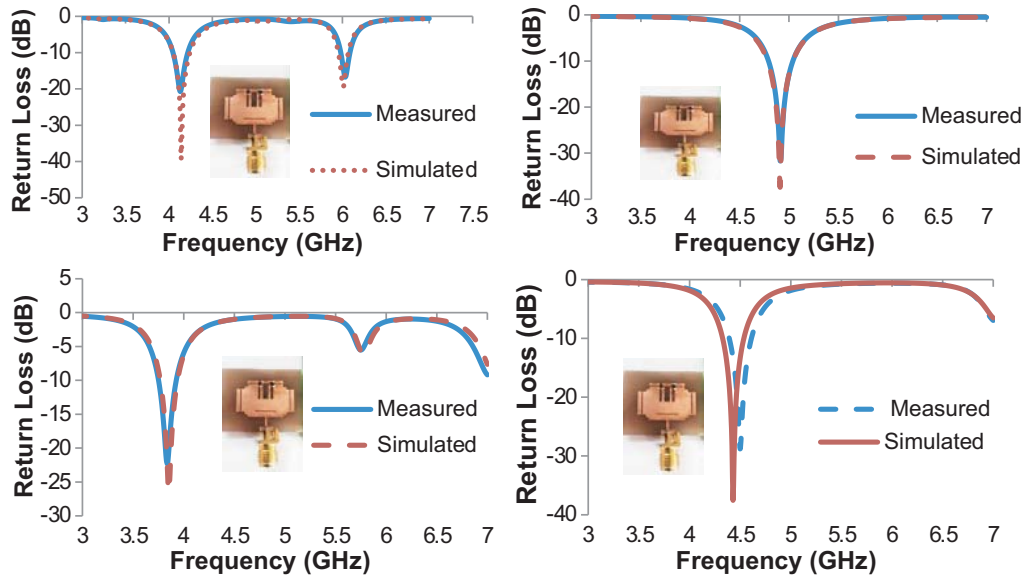


Figure 8. Simulated and measured reconfiguration responses at different switching.

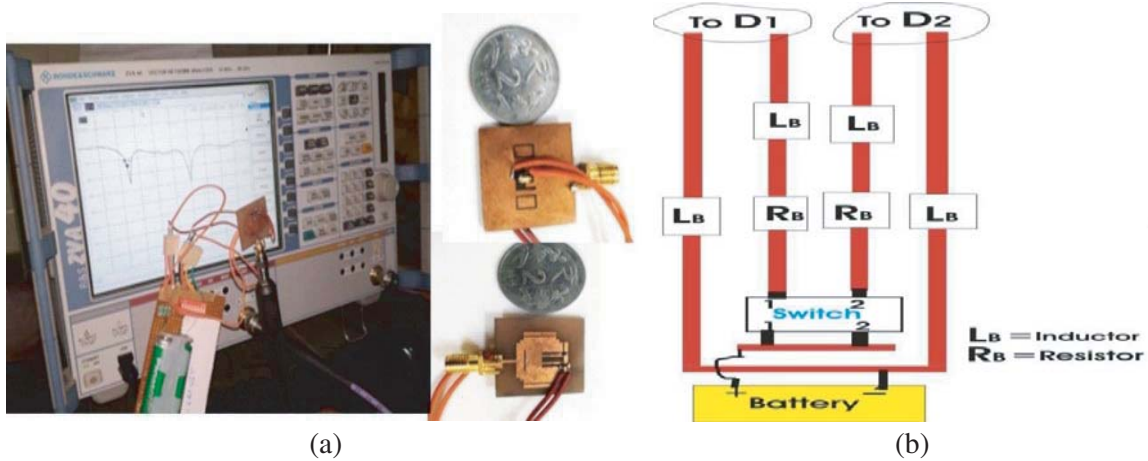


Figure 9. (a) Experimental setup. (b) Biasing circuit model.

$$L = \frac{X_L}{2\pi f} \tag{3}$$

$$L = \frac{2500}{2\pi \times 3.8 \times 10^9} = 104.76 \times 10^{-9} = 104.76 \text{ nH} \tag{4}$$

Thus an inductor of 100 nH (Murata) is used in the biasing circuit connected to the PIN diode. A resistor of 1.2 kΩ has also been inserted to limit the DC voltage across the diode. The layout of the biasing circuit is shown in Figure 9(b) with inductors L_B and resistors R_B . However, surface mount device (SMD) PIN diode has low radiation impedance characteristics as per available datasheet of BAR 50-02 V with variation of resistance from ON to OFF as 3 ohm to 3 kohm. This additional dc bias circuit maintains the radiating energy of main device and sustains the antenna key parameters from deviation during switching transition. All the parameters are compared with respect to switching of PIN to observe reconfigurability of the antenna structure.

An antenna must exhibit circular polarization as a necessary condition to become effectively operational in internet of things applications. The main beam directions indicate the orientation free

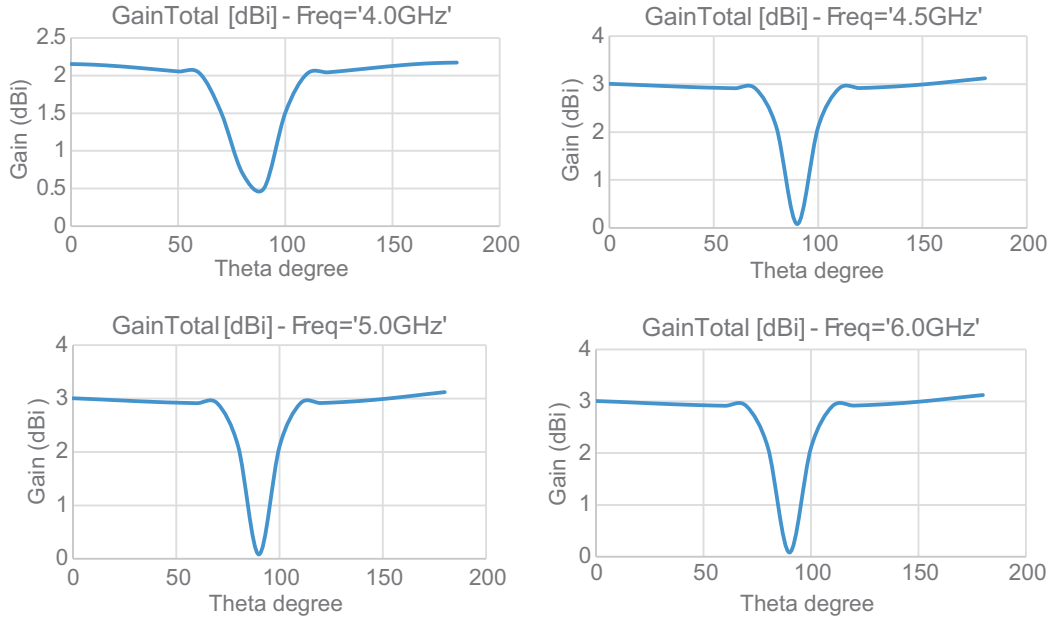


Figure 10. Main beam directions.

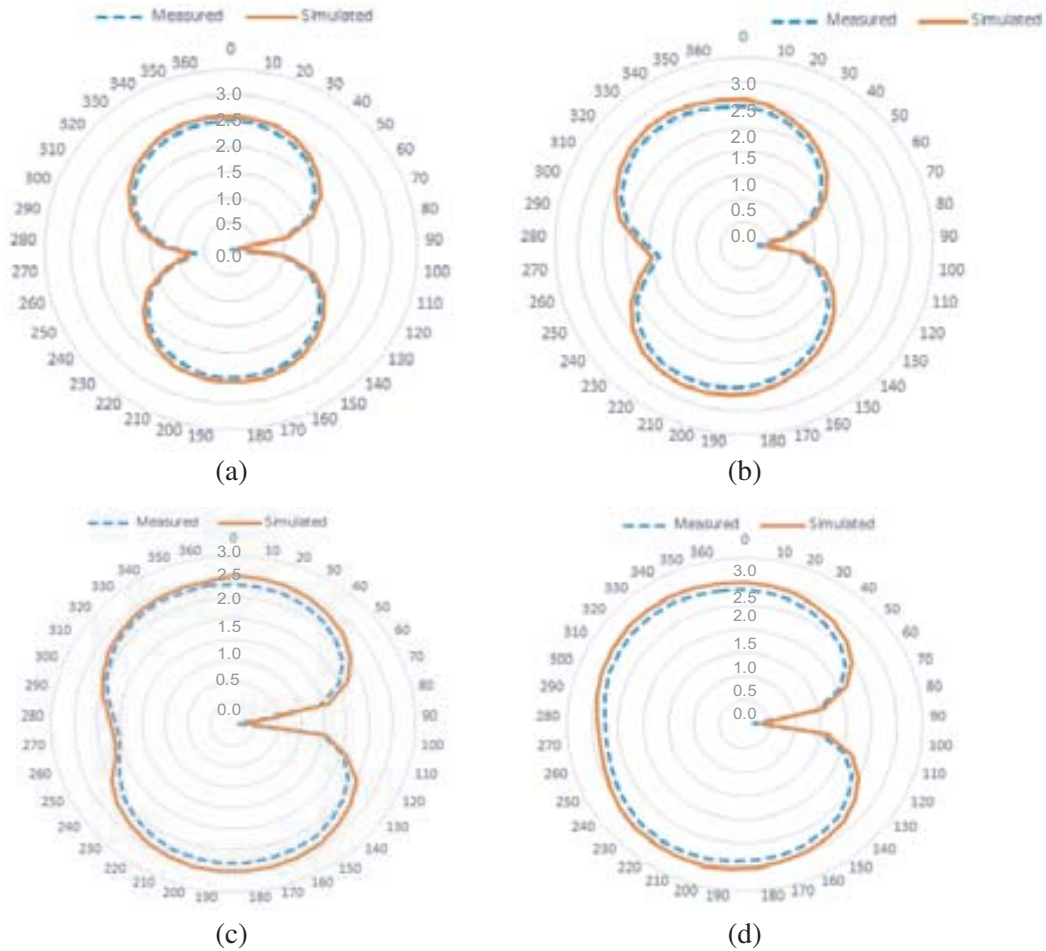


Figure 11. (dB) Simulated *E*-plane radiation patterns (a) at 4.14 GHz, (b) 6.01 GHz, (c) 4.91 GHz, (d) 3.85 GHz.

surface of the structure as shown in Figure 10. At center frequencies 4.0, 4.5, 5.0, and 6.0 GHz of the reconfiguration bands, the antenna exhibits stable gain (2.14–3.00 dBi) with respect to orthogonal main beam direction to antenna surface. This exhibits the practical implementation of the proposed structure for extensive applications in the cited frequency bands. Both *E*-plane and *H*-plane radiation patterns show stable characteristics for the entire operating band as shown in Figures 11 and 12.

The summarized results in all modes of diodes are shown in Table 6. In series of justification of novelty of the proposed antenna, the antenna is compared with other previously reported antennas as

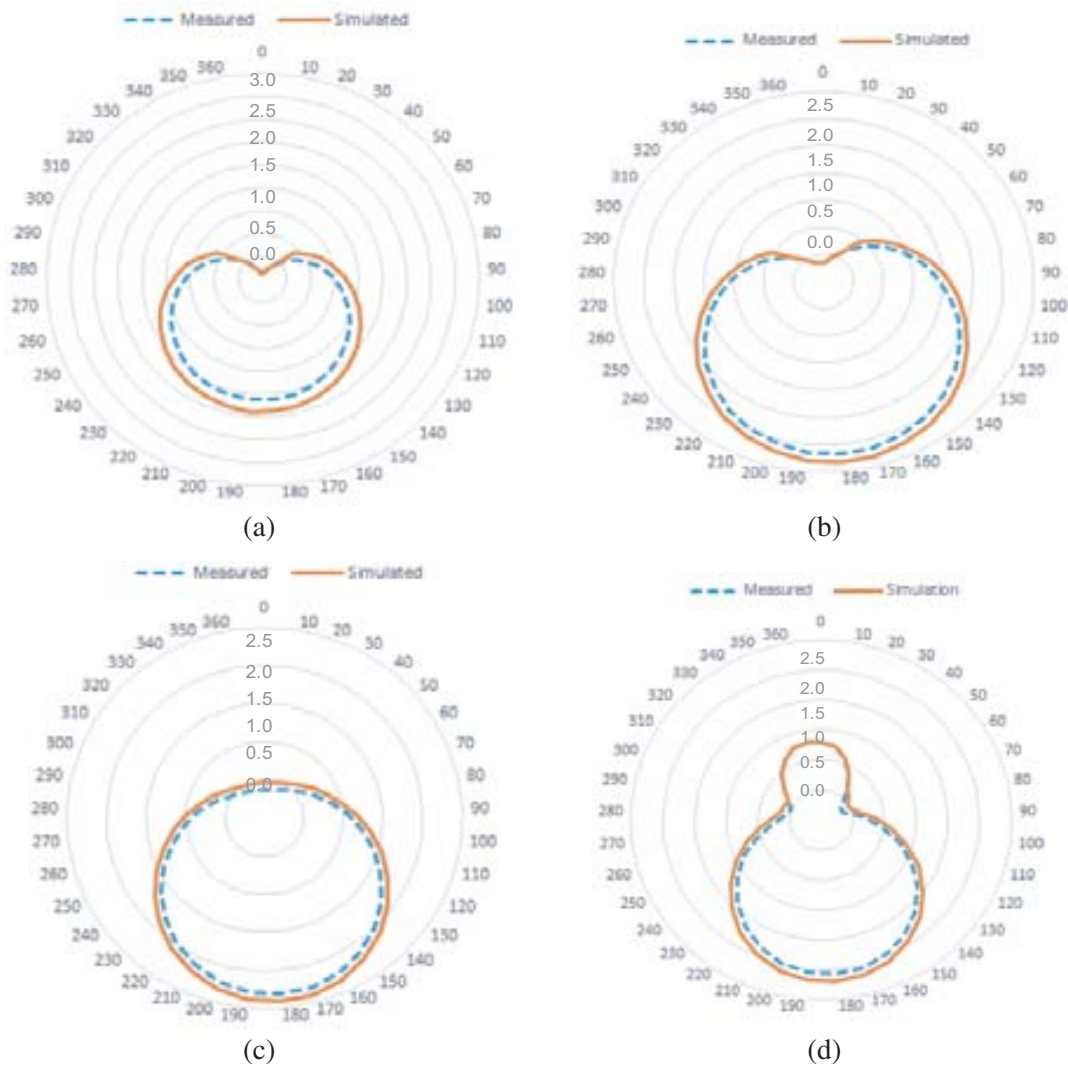


Figure 12. (dB) Simulated *H*-plane radiation patterns (a) at 4.14 GHz, (b) 6.01 GHz, (c) 4.91 GHz, (d) 3.85 GHz.

Table 6. Simulated and measured results.

Case	Frequency (Simulated)	Frequency (Measured)	Gain
000	4.14, 6.01 GHz	4.11, 6.04 GHz	2.90 dB, 3.01 dB
001	4.91 GHz	4.90 GHz	4.42 dB
110	3.85 GHz	3.82 GHz	2 dB
111	4.43 GHz	4.48 GHz	2.50 dB

Table 7. Design validation for frequency reconfiguration.

[Ref.]	Technique	Size (mm ²)	Switch Device	PIN Diodes No.	Frequency Range (GHz)	Remark
[4]	W and inverted U shaped	50 × 60	PIN	3	0.9–3.5	Large Size and Low range
[5]	Polarization switching	48 × 50	PIN	2	5.08–5.18	Large Size and Low range
[6]	Lumped elements	33 × 16	PIN	3	2–5.18	Large Size and Low range
[7]	CPW fed	25 × 31	PIN	2	2–5.5	Large Size and Low range
[11]	Six pin diode with 36 states	40 × 40	PIN	6	2.36–3.44	More No. of switching device
[12]	Bias Tee	35 × 47	PIN	1	2.5, 5.9	Large Size and Low range
[20]	Truncated elliptical radiator	40 × 38	PIN	3	2.47, 3.42, 7.18, 8.4, 12.14	Large Size and Low range
This Work	Truncated, slotted and parasitic strips	25 × 25	PIN	3	3.82, 4.11, 4.48, 4.90, 6.04	Compact with five bands

shown in Table 7. This validates the uniqueness of the design and acclaimed performance properties.

Therefore, this paper explains the proposed antenna's candidature for real time practical application in wide operating range. The designed antenna is compared with previous and recently published articles of reconfigurable antennas in Table 7. As given in the table, the designed antenna is small in size, i.e., more compact, uses fewer PIN diodes, operates over more bands, and is suitable for wireless communication.

4. CONCLUSION

The proposed antenna structure consists of two functional phenomena, one slotted symmetry with parasitic loading and the other combinational PIN diode switching. The corner truncation helps to achieve circular polarization to make face orientation free. Three PIN diodes switching in appropriate combinations generates adequate frequency shift without loss of other parametric properties. The antenna operates over a wide frequency range from 3.85 GHz to 6.01 GHz. There are four combinations of diodes, and the antenna operates on five different frequencies 3.82, 4.11, 4.48, 4.90, and 6.04, respectively. The biased switching makes the antenna highly sustainable for frequency reconfiguration and viable for multiple applications from a common structure. Also, the antenna exhibits sustained radiation properties for the complete band of operation. The antenna structure offers average 2.5 dBi gain for the entire band of operation. This results in validation and feasibility of antenna utility in multifold IoT based applications in WLAN, Wi-Max, and C-band standards.

ACKNOWLEDGMENT

I would like to thank to Rajasthan University, Jaipur for providing antenna testing facility.

REFERENCES

1. Mabaso, M. and P. Kumar, "A dual band patch antenna for Bluetooth and wireless local area networks applications," *International Journal of Microwave and Optical Technology*, Vol. 13, No. 5, 393–400, Sept. 2018.
2. Zahraoui, I., J. Zbitou, A. Errkik, E. Abdelmounim, and A. Mediavilla, "A novel printed multiband low cost antenna for WLAN and WiMAX applications," *International Journal of Microwave and Optical Technology*, Vol. 11, No. 4, 237–244, Jul. 2016.
3. Chandra, K., M. Satyanarayana, and K. Battula, "A novel miniature hexagonal shape switched pattern and frequency reconfigurable antenna," *International Journal of Communication System*, Vol. 33, No. 5, 1–8, Sept. 2019.
4. Chattha, H., M. Hanif, X. Yang, I. Rana, and Q. Abbasi, "Frequency reconfigurable patch antenna for 4G LTE applications," *Progress In Electromagnetics Research M*, Vol. 69, 1–13, 2018.
5. Singh, R., A. Basu, and S. Koul, "Reconfigurable microstrip patch antenna with switchable polarization," *IETE Journal of Research*, 10.1080/03772063.2018.1510346, Aug. 2018.
6. Shah, I., S. Hayat, A. Basir, M. Zada, S. Shah, and S. Ullah, "Design and analysis of a hexa-band frequency reconfigurable antenna for wireless communication," *International Journal of Electronics and Communications*, Vol. 98, No. 1, 80–88, Jan. 2019.
7. Chaouche, Y., I. Messaoudene, I. Benmabrouk, M. Nedil, and F. Bouttout, "A compact CPW-fed reconfigurable fractal antenna for switchable multiband systems," *IET Microwaves, Antennas & Propagation*, Vol. 13, No. 1, 1–8 Jan. 2019.
8. Gu, H., J. Wang, L. Ge, and L. Xu, "A reconfigurable patch antenna with independent frequency and polarization agility," *Journal of Electromagnetic Waves and Applications*, Vol. 33, No. 1, 31–40, Sept. 2018.
9. Patel, S., K. H. Shah, and Y. Kosta, "Frequency reconfigurable and high-gain metamaterial microstrip-radiating structure," *Waves in Random and Complex Media*, Vol. 29, No. 3, 523–539, 2018.
10. Ali, T. and R. Biradar, "A compact hexagonal slot dual band frequency reconfigurable antenna for wlan applications," *Microwave and Optical Technol. Lett.*, Vol. 59, No. 4, 2017.
11. Boukarkar, A., X. Lin, Y. Jiang, and X. Yang, "A compact frequency-reconfigurable 36-states patch antenna for wireless applications," *IEEE Antennas and Wireless Propag. Lett.*, Vol. 17, No. 7, 1349–1353, Jul. 2018.
12. Tariq Chattha, H., N. Aftab, M. Akram, N. Sheriff, Y. Huang, and Q. Abbasi, "Frequency reconfigurable patch antenna with bias tee for wireless LAN applications," *IET Microwaves, Antennas Propagation*, Vol. 12, No. 14, 2248–2254, Nov. 2018.
13. Zehforoosh, Y. and M. Rezvani, "A small quad-band monopole antenna with folded strip lines for Wi-MAX/WLAN and ITU applications," *Journal of Microwaves, Optoelectronics and Electromagnetic Applications*, Vol. 16, No. 4, 1012–1018, Dec. 2017.
14. Cai, Y., K. Li, Y. Yin, S. Gao., H. Wei, and L. Zhao, "A low-profile frequency reconfigurable grid-slotted patch antenna," *IEEE Access*, Vol. 6, 36305–36312, Jun. 2018.
15. Madi, M., M. Al-Husseini, and K. Kaban, "Frequency tunable cedar-shaped antenna for Wi-Fi and Wi-MAX," *Progress In Electromagnetics Research Letters*, Vol. 72, 135–143, 2018.
16. Goswami, P. K. and G. Goswami, "Trident shape ultra-large band fractal slot EBG antenna for multipurpose IoT applications," *Progress In Electromagnetic Research C*, Vol. 96, 73–85, 2019.
17. Gangwar, S., K. Gangwar, and A. Kumar, "A compact modified hexagonal slot antenna for wideband applications," *Electromagnetics*, Vol. 38, No. 6, 339–351, 2018.
18. Han, L., C. Wang, X. Chen, and W. Zhang, "Compact frequency reconfigurable antenna for wireless applications," *IEEE Antennas and Wireless Propagation Letters*, Vol. 15, No. 1, 1795–1798, Jun. 2018.
19. Goswami, P. K. and G. Goswami, "Truncated T-parasite staircase fractal U-slot antenna for multiple advance internet of things applications," *Microwave Optical Technology Lett.*, Vol. 62, No. 2, 830–838, Oct. 2019.

20. Allam, V. K., B. T. P. Madhav, T. Anilkumar, and S. Maloji, "A novel reconfigurable band-pass filtering antenna for IoT communication applications," *Progress In Electromagnetics Research C*, Vol. 96, 13–26, 2019.
21. Romputtal, A. and C. Phongcharoenpanich, "Frequency reconfigurable multiband antenna with embedded biasing network," *IET Microwaves, Antennas & Propagation*, Vol. 11, No. 10, 1369–1378, 2017.